

## AN EXPLORATORY STUDY ON THE ACCURACY OF PARTS PRINTED IN FDM PROCESSES FROM NOVEL MATERIALS

Halina NIECIAŁ, \* Rafał KUDELSKI, \* Piotr DUDEK, \* Jacek CIEŚLIK\*

\*Faculty of Mechanical Engineering and Robotics, Department of Machine Design and Technology, AGH University of Science and Technology, Al. Adama Mickiewicza 30, 30-059 Kraków, Poland

[hnieciag@agh.edu.pl](mailto:hnieciag@agh.edu.pl), [kudelski@agh.edu.pl](mailto:kudelski@agh.edu.pl), [dudek@agh.edu.pl](mailto:dudek@agh.edu.pl), [cieslik@agh.edu.pl](mailto:cieslik@agh.edu.pl)

received 25 October 2019, revised 24 April 2020, accepted 28 April 2020

**Abstract:** The paper describes the experiment of assessing the chosen geometric characteristics of test models with simple geometry, shaped by the FDM (fused deposition modelling) method of different materials. The influence of the material grade and the degree of infill density on the shrinkage affecting their dimensional deviations and selected surface topography parameters of printed parts was examined and compared. Three different types of materials were used to fabricate the test models, namely HDGLASS and NANOCARBON, two new fibre reinforced composites available in the market and, additionally ABS, a popular monoplasic material. An infill density ratio of 10, 50 and 90% was assumed for each material. Three specimens were made on the same printer for each infill density, which allowed to assess the repeatability of the analysed characteristics. From among many possible shapes of models, a cube was chosen as representing the simplest geometry, facilitating the measurements themselves and the interpretation of the results. New fibre-reinforced materials are more attractive in industrial applications than pure plastics (ABS) due to their mechanical properties or appearance. They are characterized by a relatively low melting point and short cooling time, after which they can return to their original geometry; however, there is a lack of detailed data on the geometric accuracy of parts made of used composite materials. The presented work was to explanatorily broaden the knowledge about the properties of composite made parts. The practical purpose of the research was that on the basis of measurements, it would be possible to indicate among the materials used that particular material whose properties and method of application would allow obtaining the best quality surface and would be the most resistant to thermal loads. An attempt was also made to explain the possible causes of the differences in the observed characteristics of the tested materials.

**Keywords:** FDM, thermoplastic filament materials, geometrical accuracy

### 1. INTRODUCTION

Additive manufacturing (AM) is a popular alternative to subtractive manufacturing and formative manufacturing methodology. Products shaped by this technology, also called as 3D printing, are made from 3D model data, usually by adding layer upon layer (ISO/ASTM 52900:2015). Frequently chosen method is the Fused Deposition Modelling (FDM) method suitable for thermoplastic materials. Its advantages include a wide choice of materials, good strength properties of the parts built, as well as a simple process model that affects the simple construction and thus low cost of FDM machines. Products shaped by AM technology are more and more often used as end-use parts or functional elements ready for assembly. Appropriate surface quality (Adamczak, 2008) and form-dimensional accuracy (PN-EN ISO 286-1: 2011) become very important and allow to eliminate the costs of finishing operations.

With the exception of universal requirements for the proper functioning, durability and reliability of the product, the desirable product properties, regardless of the technology, are mainly due to its intended use.

The quality of the product is therefore conditioned by the characteristics related to the individual desired properties, so quality level is formed by three main factors: (1) product design; (2) material; (3) parameters and conditions of the manufacturing process (Bähr and Westkamper, 2018).

#### 1.1. Project phase

For both end-use parts and parts that are elements of assemblies, a set of characteristics consisting of the specification established in the design phase is important. These are geometrical features, surface topography, concerning topological aspects of surfaces and the structure of the surface layer. These three attributes of the correct part geometry have been extensively studied for parts manufactured in conventional subtractive processes, based mainly on machining. Material removal process has a strong influence on the topological and structural changes to machined surfaces. Irregularities and deformations of the machined surface occur due to the existence of cutting forces and friction of the cutting tool while machining.

Topography and surface texture is considered the most important geometric feature among the geometric quantities and parameters describing the surface structure after shaping (Petropoulos et al., 2010). As numerous works have found, the condition of surface could directly affect the functional features of the product. In Hashimoto et al. (2016), the influence of surface characteristics after four types of fine-finishing on functional characteristics, including tribological parameters and stress, was examined. The relationship between the state of the surface and wear resistance, sealing properties and corrosion resistance of parts and fatigue was concluded in Zabala et al. (2018).

With the appearance of new technologies like AM, there was

a necessity to verify these dependences.

The geometry of the parts fabricated in 3D printing processes, as opposed to machining, is created additively by adding material. In the FDM method, the surface condition with a characteristic texture is also formed by various phenomena accompanying the cooling process, affecting the properties, structure and thermal stress of the material.

Until recently, in industrial practice, surface texture was treated as an indicator of process variability (e.g., due to tool wear or machine vibration). In case of a stable process,  $R_a$  – the basic 2D parameter – characterizing the roughness and surface texture quite well. In practice, most surface roughness tests are still based on profile measurements and 2D parameters, which have been well recognized. As discussed by Guillemot et al. (2014), 2D parameters are an important indicators of product and process quality, but insufficient, for example, for complex surface texture or its anisotropy. Meanwhile, in the case of FDM method, the surfaces exhibit a clear anisotropic, nonuniform texture; therefore, the way of measurement should be chosen to fully characterize and describe them (Triantaphyllou et al., 2015).

Modern surface metrology is increasingly referring to spatial measurements (Guillemot et al., 2014; Mathiaa et al., 2011; Singh and Vatsalya, 2015) and topographic characteristics as surface descriptors, which represent the state of the entire surface, not just its cross-section.

The knowledge of relationships between 2D/3D parameters versus functional parameters of parts produced by finishing machining allows predicting and obtaining the products with improved functional properties (Grzesik, 2016). According to the author, the knowledge of topography can be employed for typical or unconventional processes to optimize the process settings or tools.

To summarize, in modern research, in the assessment of the quality of AM surfaces, three directions can be distinguished:

- determining the relationships between surface quality and desired surface function;
- selection and measurements of a representative characteristic or set of surface characteristics;
- optimization of process settings to establish the best surface quality.

Relatively little studies have been found in subject literature considering nothing except the issue of dimensional and form accuracy. These include the work by Spoerk et al. (2019), where the properties of (PP) semi-crystalline polypropylene composites processed by SLS method were analysed. A simplified stress deformation model has been developed for the purpose of warp analysis (Wang et al., 2007). In other studies, only certain geometrical features were inspected as one of the others quality indicators of FDM fabricated parts (Alsoufi and Elsayed, 2018; Nuñez et al., 2015; Tomić et al., 2017; Umaras and Tsuzuki, 2017).

## 1.2. Material and its composition

Material is an important factor affecting the quality of a product fabricated by AM technology. Building material (a filament) is used nowadays, instead of classical materials from the group of metals or ceramics, as a construction material, whose geometric (type and diameter of filament) and technological properties (high strength, combined with low density) depend on the geometrical and mechanical properties of the product. It is not easy to choose the best material to meet the construction and strength require-

ments in a given application, and at the same time, take this important aspect of product suitability into account.

Thermoplastic filament materials commercially available in the consumer market are fabricated commonly from acrylonitrile butadiene styrene (ABS), polypropylene (PP), polycarbonate (PC), polylactic (PLA), polyether (PEI), and others (Ligon et al., 2017). Traditional mono-plastics are now more and more often replaced with composites and nanocomposites. They are formed on the basis of a polymer matrix with the addition of inorganic fillers in order to improve their mechanical, optical, electrical and thermal properties. These can be glass fibres, carbon fibres, calcium carbonate, talc and many more. In recent years, progress at AM is mainly associated with the development of new materials that will enable 3D printing of parts with better mechanical performance and quality (Roberson et al., 2015).

The latest research trends towards developing techniques for the production of new fibre reinforced polymer composites (ranging from nanoscale discontinuous to continuous fibres) are described in (Duo Dong Goh et al., 2019). Recent achievements and technologies in this field are presented, as well as a list of materials with their advantages and disadvantages. Other current work in this field (Hofstätter et al., 2019) discusses the problems of composite production, the effect of fibre length, their orientation, the share of additives in polymer matrix on the composite properties and requirements for its processing. This publication also provides an overview of the materials currently available in fibre reinforced materials technology. The final desired properties of a composite depend on not only the properties of its components, but also many factors associated with its fabrication, which is why the development of an appropriate technology becomes an important problem that is analysed in many works. Mohan et al. (2017) makes an extensive review on the fabrication methods of specimens using various composite materials and optimization of their processing parameters in the FDM method to improve various mechanical properties and other desirable properties of 3D printed parts.

Carbon fibres are the common polymer additives. The importance of carbon fibres to additive manufacturing owes to such advantages as low weight, high tensile strength and low thermal expansion (Al-Hariri et al., 2016). Techniques for reinforcing polymers are presented in the paper, among others by using two separate printheads, the first of which dispenses the polymer, such as nylon or PLA, while the second the carbon fibres.

Blok et al. (2018) investigates the impact of carbon fibre architecture in composites on mechanical properties (tensile strength and stiffness) and so-called processability (including melt viscosity, temperature, thermal conductivity, and others).

As a result of the research (Kaczyński et al., 2014), the wear mechanism of thermoplastic composites reinforced with unidirectional carbon fibres was found to increase strength and wear resistance. The authors state the possibility of using the height of fibres reinforcing the polyamide matrix and their angle of orientation to predict the wear resistance. The authors (Prusinowski and Kaczyński, 2017) are investigating the possibility of achieving the desired properties through the use of an appropriate extrusion head design in the FDM method by orienting reinforcing carbon fibres of the appropriate length. Another work (Roberson et al., 2015) demonstrates the production of composite materials for AM based on FDM technology, aimed at obtaining the properties expected in given electromagnetic and electromechanical applications. It is also possible as authors state to reduce disadvantageous features such as anisotropy of mechanical properties, as

well as consideration of an important aspect of surface finishing.

Research is also ongoing regarding the usage of glass fibres in polymer matrix (Duo Dong Goh et al., 2019). Experiments involving a composite based on Nylon 6 with various admixtures of glass fibres, described in the study by Kumar and Panneerselvam (2016), reveal a significant increase in abrasion resistance as the fibres' content in the composite increased. Along with the glass fibres' share, the wear indicator decreases and is the lowest at 30% glass fibres. The addition of glass fibres also reduces plastic deformation, and its dispersion in the matrix improves tensile strength and hardness.

### 1.3. Material extrusion process

The final quality of the 3D printed object is also affected by the speed of extrusion, bed and printing head temperature, nozzle diameter, ambient temperature, and slicer parameters (algorithm forming layers of the model), such as wall thickness, type of filling and so on (Calcagnile et al., 2018; Mohan et al., 2017; Umaras and Tsuzuki, 2017). Taking into account such a large number of factors influencing the process, the preparation of test artefacts is a common practice (Knoop et al., 2018; Liua et al., 2019; Spoerk et al., 2019), on the basis of which, it is possible to carry out tests and determine the effect of processing condition on the quality of the products.

An important aspect of producing high quality products is the cost of obtaining it (Dudek and Zagórski, 2017). A way to reduce the costs of producing FDM products is to shorten processing time and minimize material waste by applying the appropriate density of laid layers, known as the degree of infill density. This parameter is characterized by the amount of material inside the volume of the 3D printed model, so when completely filled with solid material, it occupies 100% of the volume; for empty (not filled with material), it is 0% (Loncierz and Kajzer, 2016).

The dynamic progress observed in the production of composite materials is often ahead of research, thanks to which one can comprehensively learn about the geometrical properties of an object affecting its functionality or appearance. Rapid changes in the composition, the innovations of polymer blends mean that with the development of new filament products, it is necessary to re-examine the manufactured part characteristics, hence predicting the accuracy – as some experts consider – is still an open issue. This problem particularly applies to commercial versions of materials, that is, filaments. There is a need to continuously broaden the knowledge on commercially available versions of composite materials (Hofstätter et al., 2019) and conducting research.

The aim of the published work was to experimentally investigate the geometrical properties of FDM manufactured parts. This paper describes the experiment of assessing the accuracy of test models with simple geometry made of three different commercial filaments. The choice of material should be made before designing the object, taking into account the desired properties of the object. Therefore, the influence that the material or the degree of infill density has on the chosen surface texture parameters of the specimen surface as well as on the shrinkage was investigated and compared.

## 2. EXPERIMENT

Three different materials were chosen for the study, which are currently of great interest to manufacturers of 3D printed products.

The first is a widely used traditional ABS polymer material, that is, acrylonitrile butadiene styrene, a completely amorphous material (<http://www.rp-tech.pl>; Nuñez et al., 2015; Żuchowska, 2000). Products made of this material are characterized by good mechanical properties and a wide range of temperatures of use. It is willingly chosen by manufacturers due to its ease of processing and relatively low price.

The next two are new composites: HDGLASS and NANOCARBON.

NANOCARBON is a polyamide (mainly PA12) with filling of carbon fibres. It is a partially crystalline composite material, characterized by excellent mechanical properties and very high chemical resistance thanks to the addition of fibres ([www.markforged.com](http://www.markforged.com)).

The third material, HDGLASS, is a new glass-like filament, made from an unique blend of PETG (polyethylene terephthalate), a material that is rapidly growing in popularity. Polymer matrix belongs to the group of polyesters that have a tendency to form a crystalline phase ([www.formfutura.com](http://www.formfutura.com)). It is particularly interesting because detailed information based on scientific research carried out is not found about the properties of this material yet. The composite is characterized by 90% light transmission, high hardness and strength, as well as high resistance to high temperatures. The part 'HD' in the filament name means 'Heavy Duty'. Its additional advantage is the fact that it is suitable for contact with food (FDA certificate).

### 2.1. Material properties

Selected thermoplastic filament materials are characterized by different melting temperature and different thermal stability (Tab. 1), which can affect the state of the material after polymerization due to temperature reduction (cooling process).

Tab. 1. 3D printing filaments – Manufacturer's specification

Material type	ABS	NANOCARBON	HDGLASS
Colour	Brilliance black	Matte black	White
Filament Diameter [mm]	0.2	0.2	1.75
Melting Temperature (the temperature of the extruder) [°C]	220 ÷ 290 (240 ÷ 270)	245 ÷ 265	215 ÷ 225 (PETG: 265)
Coefficient of Linear Thermal Expansion [m/m x °K]	7.38 x 10 <sup>-5</sup>	No data (PA12: 12 ÷ 14 x 10 <sup>-5</sup> )	No data (PETG: 8 ÷ 10 x 10 <sup>-5</sup> )
Density [g/cm <sup>3</sup> ]	1.03 ÷ 1.05	1.02 ÷ 1.24	1.270 (PETG:1.4)
Young's Modulus E [MPa]	1900 ÷ 2600	2700 ÷ 7600	2147.6
Tensile Strength Rm [MPa]	34 ÷ 51	41 ÷ 165	No data
The Temperature of Product Use [°C]	-40 ÷ 85	-30 ÷ 80	No data

### 2.2. 3D printer

The test specimens were made on the PRUSA ORIGINAL i3 machine, with working range 250x210x200 mm (Fig. 1a). It is one of the most popular printer models.

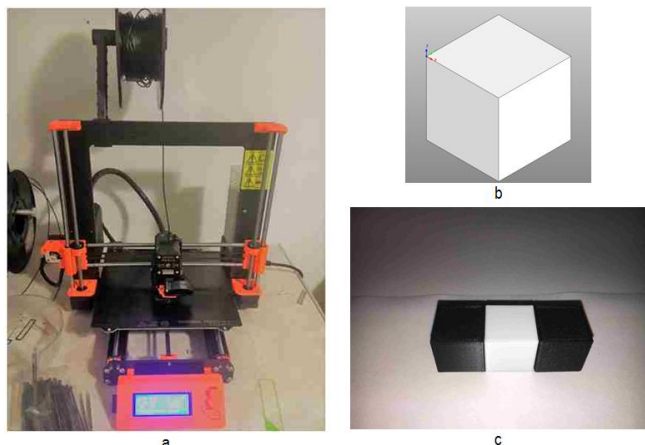


**Fig. 1.** Specimens manufacturing a) FDM machine; b) Printed model; c) Test specimens with different filament materials

According to users, this model combines good price with good print quality. The printer is equipped with a magnetic bed with the possibility of automatic levelling of the heating bed. The printer's advantages include a wide range of materials that can be used at work, from the most popular, such as ABS, to fibre reinforced composites.

### 2.3. Tested specimens

The specimens had the shape of a cube (Fig. 1b; Fig. 1c) with dimensions of 20x20x20 mm. The shape and dimensions of the tested specimens are important in determining mechanical properties while strength tests (Dikshit et al., 2017). Among many models, a cube was chosen as representing the simplest geometry, shortening time and facilitating the measurement and interpretation of results regarding geometric accuracy. For each material tested, three specimens were manufactured with a cross-fill rate (infill density) of 10%, 50% and 90%, which means that the material inside the cube, which forms the grid, occupies 10%, 50% or 90% of the internal volume. The 3D model was developed in Autodesk Inventor 2019 and then a G-Code was generated with Simplify 3D to control the printer. Tested specimens were printed at different extruder temperatures, bed temperatures and feed rates. The parameter values recommended by the machine manufacturer for the given material were used to ensure the correctness of process flow and good results. The levels of main process parameters are shown in Table 2.

**Tab. 2.** Factors settings of process 3D printing

Material	Nozzle temperature [°C]	Bed temperature [°C]	Printing speed [mm/s]
ABS	250	100	80
NANOCARBON	240	50	70
HDGLASS	210	90	65

The material consumption of each produced specimen was determined on the basis of weighing by AXIS electronic analytical balance. The device has a measuring range of 200 g and resolution 0.001 g. Table 3 below shows the average weight of three samples of each material.

Specimens were fabricated within two days at a constant am-

bient temperature, using a filament from a single roll. They were then naturally cooled to room temperature of  $25 \pm 1^\circ\text{C}$ .

**Tab. 3.** The specimens mass

Filament material/infill density	The average specimen mass $10^{-3}[\text{kg}]$		
	10%	50%	90%
ABS	3.744	5.842	7.714
NANOCARBON	3.467	5.308	6.905
HDGLASS	4.826	7.254	9.449

All specimens were made with the same nozzle diameter. The thickness of the printing layer was set to 0.2 mm and was a constant for all specimens.

## 3. MEASUREMENTS

### 3.1. Measuring instrumentation stand

After the specimens were fabricated, the surface quality assessment was carried out on the basis of the chosen roughness parameters and areal surface parameters as well. Surface measurements were carried out using two methods: linear profiling (PN-EN ISO 4287: 2010; PN-EN ISO 4288: 1997) and spatial topography (ISO 25178-6:2011; Wieczorowski, 2013).

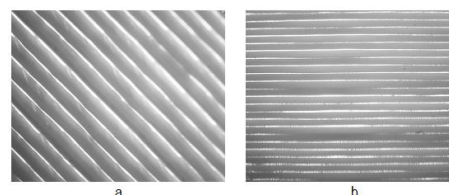


**Fig. 2.** Texture direction on: a) The top face of the cube; b) The side face of the cube

Figure 2 shows a microscopic representation of the structure of the upper face (a) and side face (b). The surface maps show typical traces of the specimen surfaces by positioning the strips of an extruded filament of a certain diameter and ovality. When applying one layer, a contour was created first and then the interior strips for each subsequent layer were rotated at 90 degrees from the previous arrangement. For the n-layer, the slope angle about the X-axis is  $-45^\circ$ , and for the n+1-layer, the same angle is  $+45^\circ$ . This arrangement of extruded filament strips shaped a surface with anisotropy texture character. This fact was taken into account in determining the cross-section of the analysed surfaces.

### 3.1. Profile roughness measurements (ISO 4285)

For roughness measurements using the profile method, FORMTRACER SV-C450 (Mitutoyo), a surface roughness/contour measuring system was used, equipped with a contact stylus (Fig. 3a). It has a measuring range of 800/800/8 um, straightness (0.5+0.001L) um, resolution 0.01/0.001/0.0001 um. Measurements were carried out on the upper surface, perpendicular to the direction of the extruded material path ('machining trac-

es'), and on each side of the cube perpendicular to the direction of the layers. Three measurements of roughness were taken on each surface except bottom face as it adheres to the base machine plate. During the profile assessment, the amplitude parameters were determined.

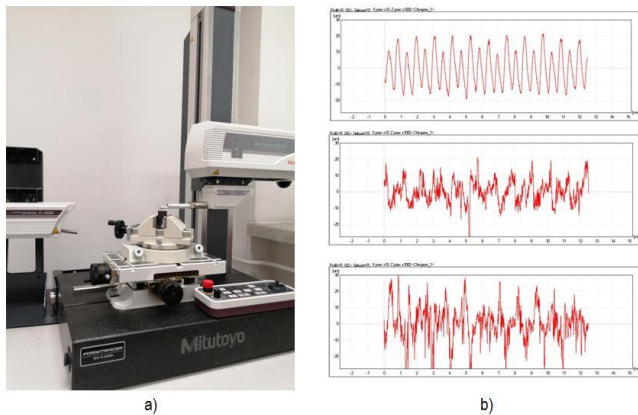


Fig. 3. Roughness measurement a) FORMTRACER SV-C450; b) Profiles of surface texture for three materials

Among others,  $R_a$  – an arithmetic mean deviation of the profile,  $R_q$  – mean square deviation of the profile,  $R_z$  – the highest height of the profile (Fig. 3b). The values of these parameters were then averaged. As a measure of the dispersion of the results obtained, the range, the difference between the largest and smallest values in the sample was considered.

### 3.2. Surface roughness measurements (ISO 25178)

Measurements of areal parameters were carried out using a contact instrument for measuring and analysing surface topography TOPO 01P IZTW, equipped with a rotational scanning table with 50x25 mm scanned area (Fig. 4a). The 3D parameters considered for analysis were following:  $S_a$  – an arithmetical mean height,  $S_q$  – root mean square height,  $S_z$  – maximum height of scale-limited surface.

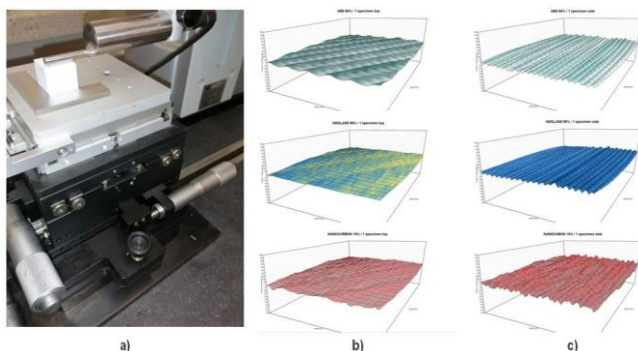


Fig. 4. Topography measurement a) Topo 01P profilometer, probe measurements range 250  $\mu$ m (S250 probe); b) Charts of surface texture of top faces; c) side faces

The measurements were performed on each surface except bottom side, as before. The obtained results – the graphs of surface topography – were analysed for top faces (Fig. 4b) and for side faces (Fig. 4c).

### 3.3. Geometric accuracy representation measurements

The dimensions and shape of the specimens had deformed due to shrinkage. There was a change in volume, created during cooling of polymeric materials and crystallization for semi-crystalline materials (Kwiatkowski and Kwiatkowska, 2012; Zawistowski, 2008).

The geometric-dimensional analysis was based on the measurements of specimen length as the distance between the central points of side walls in the X (1) and Y (2) directions and in the Z direction (3) – the direction of application of layers as the distance between the upper and bottom surface of the specimen. Mitutoyo 0.1/150 mm, MPe = 0.02 mm, the electronic calliper was used for measurements. The accuracy measure were deviations of the dimensions observed from the dimensions of the programmed model. The results of the measurements were averaged for each test case and the range in the observed values was taken as a measure of dispersion.

## 4. RESULTS

The experimental scenario excluded a comparative analysis of the results obtained, because the specimens were not formed in equivalent processes. For each series of three specimens, the optimal, but slightly different, set of process parameters for the specified material was applied. Furthermore, different measuring instruments were used to measure the specimens and the surface texture parameters were determined by their (different) software. Therefore, the obtained data do not meet the conditions of repeatability necessary for traditional analysis.

The analysis, therefore, focused on the comparison of the degree to which materials react to the phenomena of surface texture formation and the phenomenon of shrinkage, a fundamental issue, for example, in plastics processing.

In the publication, one restrained to presenting only two but commonly used parameters, that is,  $R_a$  and  $S_a$ .

Parameter  $R_a$  – arithmetical mean deviation of the assessed profile – is an arithmetic mean of the absolute ordinate values  $z(x)$  within a sampling length  $l$  (1).

$$R_a = \frac{1}{l} \int_0^l |z(x)| dx \quad (1)$$

For the characterisation of surface texture, the areal parameter  $S_a$  was used (2), that is, an arithmetic mean of the absolute of the height within a definition area (A).

$$S_a = \frac{1}{A} \iint_A |z(x, y)| dx dy \quad (2)$$

Unlike in other processes using thermoplastic materials, for example, during injection moulding, it was not possible to determine the processing shrinkage as a share of the product volume in the volume of the injection mould used to make it. In this paper, deviations  $\delta$  from the dimension imposed by the design were analysed and linear (longitudinal) shrinkage was calculated according to Formula (3).

$$S_l = \frac{l_o - l}{l_o} = \frac{\delta}{l_o} \quad (3)$$

where:  $S_l$  – the value of the deviation in the selected direction (x, y, z),  $l_o$  – length of the model in the selected direction,  $l$  – observed dimension.

4.1. Roughness of surface texture

The differences in roughness are illustrated by the graphs of the  $R_a$  parameter (1), for the side faces (Fig. 5a) and upper faces of the specimens (Fig. 6a).

The graphs show that the roughness and topography of the side faces (Fig. 5a) for a specific material are stable for different degrees of infill density and the values of the surface texture parameters are slightly differentiated. The highest values have been noticed for NANOCARBON composite and the lowest values for HDGLASS.

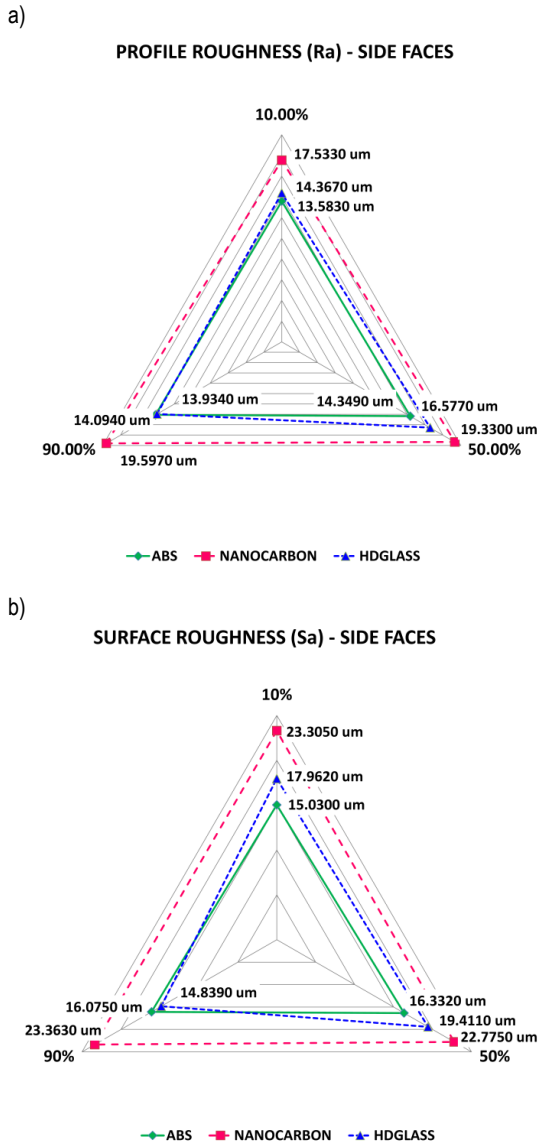


Fig. 5. Roughness parameters versus infill density (%) for side faces: a)  $R_a$  [um]; b)  $S_a$  [um]

A similar relation can be observed when analysing the upper surface on which the layers have been laid. The NANOCARBON surface turned out to be the least smooth, while for the remaining two materials (ABS and HDGLASS), the measured surface irregularities were smaller. This is probably due to the presence of carbon fibres in the NANOCARBON material, which produce a roughness effect felt by the fingers.

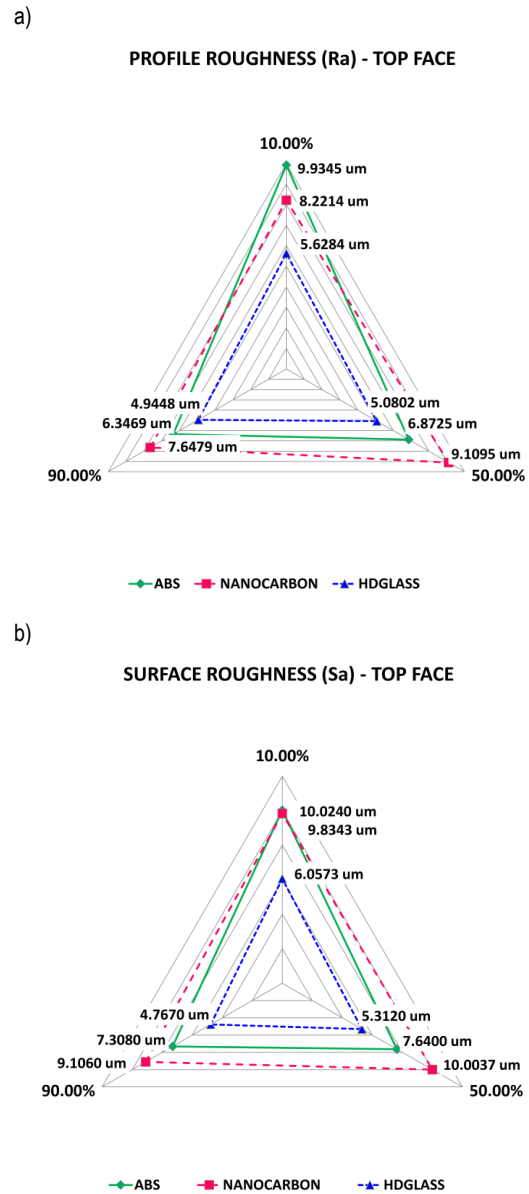


Fig. 6. Roughness parameters versus infill density (%) for top faces a)  $R_a$  [um]; b)  $S_a$  [um]

The view of intensity images captured by Marsurf CM Expert focus microscope show the difference between surface structures of the two composites (Fig. 7). There was a large difference between the surface texture parameters of the side faces and the upper face, which was much less uneven. The biggest difference was observed for HDGLASS composite.

However, additionally, an interesting observation was the different effect of the infill density on the roughness of the materials. HDGLASS material was characterized by similar  $R_a$  values, regardless of the infill density, and the ABS material turned out to be the most sensitive to the infill density (increasing the level of infill density from 10% to 90% reduces the  $R_a$  parameter about 1.6 times).

The topography of the surface was also evaluated on the basis of amplitude areal parameter (2), for the side faces (Fig. 5b) and upper faces of the specimens (Fig. 6b). The values in relation to the profile parameters were generally higher, which could be a consequence of the enlargement of the area (surface areas) for

which they were determined, that is, the fact that the measurement of the profile did not take into account any irregularities situated outside the chosen cross-section.

However, the ratio of the values of surface parameters to profile parameters was different for the three materials. For NANOCARBON material, the surface parameters were about 19% higher than the profile parameters; for other materials, the differences were smaller (for ABS did not exceed 15%, for HDGLASS was less than 10%).

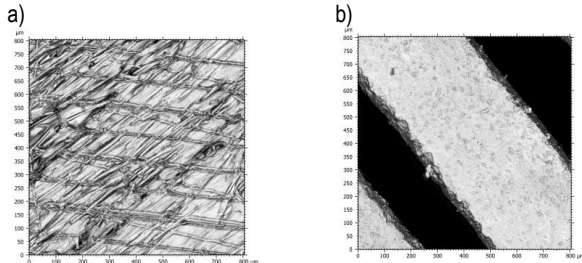


Fig. 7. Intensity image of: a) NANOCARBON; b) HDGLASS

The graph in Figure 8 illustrates an important argument proving the validity of multi-parametric evaluation by extending the set of profile parameters by 3D parameters of surfaces shaped in the FDM technology.

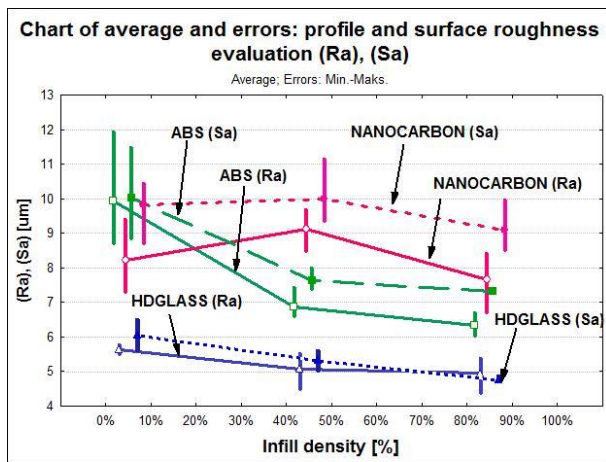


Fig. 8. Summary analysis results of profile and surface roughness measurements for the three types of filament material

The observation of the curves shows that in all the studied materials, the profile evaluation results in a larger dispersion of parameters, while the spatial parameters have a smaller dispersion. The dispersion characterizes in fact the actual variation of irregularities of the surfaces due to factors such as unstable values of process parameters. The smallest change in process parameters may lead to a change in product properties, but noticeably higher values of profile parameters range in relation to spatial parameters spread may be the result of the method of measurement and imprecise determination of the direction of measurement of the texture having clear anisotropy features.

#### 4.2. Dimensional deviations by thermal affects

The measured dimensional deviations are shown in the diagrams in Fig. 9 and Fig. 10.

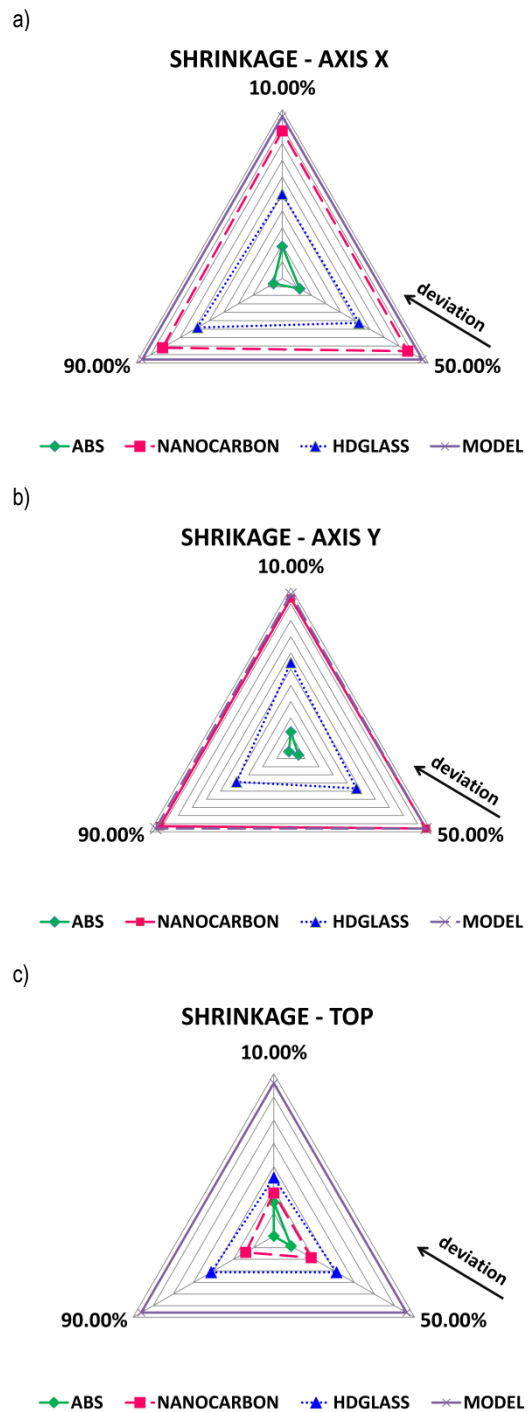


Fig. 9. Effect of type of filament material on thermal deviations  $\delta$  [mm] for: a) X axis; b) Y axis; c) Z axis

As the dimensions of the 3D model are the same for all specimens, they represent the same tendency as linear shrinkage (3).

The dimensional deviations of the side surfaces for composite materials are evenly distributed in X, Y and Z directions (all three axes of the printer) for all density levels. The situation is different with ABS material. In accordance with the tendency for processing shrinkage reported by Nuñez (2015), the specimens made of this material were characterized by negative dimensional deviations on the lateral surfaces and at the same time, there was seen a visible dependence of shrinkage on the infill density. At 90% level (in case of almost full model), the dimensional accuracy deter-

mined by a negative deviation from the model dimension is the worst. For the highest density of the upper surface, the linear contraction was almost 0.73%.

5. DISCUSSION

It should be noted that the research was concerned with two groups of materials: amorphous thermoplastic and composites based on semi-crystalline material matrix. Investigating the material properties but in another process, that is, injection moulding process (Kwiatkowski and Kwiatkowska, 2012; Zawistowski, 2008), the authors drew that thermoplastics, partly crystalline (1÷5%), have higher shrinkage values, while amorphous thermoplastics (0.3 ÷ 1%) have smaller ones, which could be explained by the arrangement of macromolecules of the structure, denser than for amorphous plastics.

However, the studies presented in this publication prove that the addition of fibres to the polymeric matrix changes this relation and improves some geometric properties of the product, as was a case with HDGLASS. The improvement consists in the reduction of shrinkage, more even distribution of shrinkage values, as well as surface texture parameters in relation to the infill density and direction, additionally in the case of composites with the addition of glass fibres, and also in the reduction of surface irregularities.

The mechanism of improving the properties of composites is complex and difficult to explain without an analysis of physical and thermal phenomena accompanying the thermoplastic materials processing. It is determined by various factors, physicochemical and viscoelastic properties. The influence of inter-phase interactions between polymer chains and fibres (Barczewski et al., 2012; Gołębowski, 2004) and the formation of new chemical bonds is also considered.

The processes of additive fused deposition for amorphous and semi-crystalline plastics are not homogeneous. Application of ABS layers requires a plastic state: viscous. Depending on the viscosity, the material is integrated along the extruder paths. Within the active layer applied, macromolecules may still partially move. As a result, the shaped surface does not reproduce the filament stripe contours because they are blurred. The resulting irregularities – in accordance with the course of the process – will depend on its parameters: among other things, the feed rate (pathway adhesion surface) and temperature reduction rate.

The process of applying layers has a different effect on the phenomenon of shrinkage.

ABS material remains amorphous in the solid state also after exceeding the glass transition temperature,  $T_g$  (Żuchowska, 2000). From the moment  $T_g$  is exceeded until the product reaches the ambient temperature, the product undergoes thermal shrinkage as a solid object. This process takes place layer by layer. The highest, near-surface layers may still be in the glass transition state, which is characterized by elasticity (characteristic for amorphous polymers), while the lower layers may already be solidified; therefore, in the cross section of the product, there are inner stresses that may simultaneously lead to contour deformations of the product such as buckling.

In the polymer matrix of composites, when the  $T_k$  crystallisation temperature is exceeded, solidification occurs by ordering the molecules and forming crystallites. These semi-crystallisation materials are characterized by the lack of elastic phase, but between  $T_k$  temperature and melting temperature, cold crystallization can occur.

The examined properties of HDGLASS composite can be then attributed to the conditions of the cooling process. The addition of glass fibres to the main polymer matrix groups hinders the free

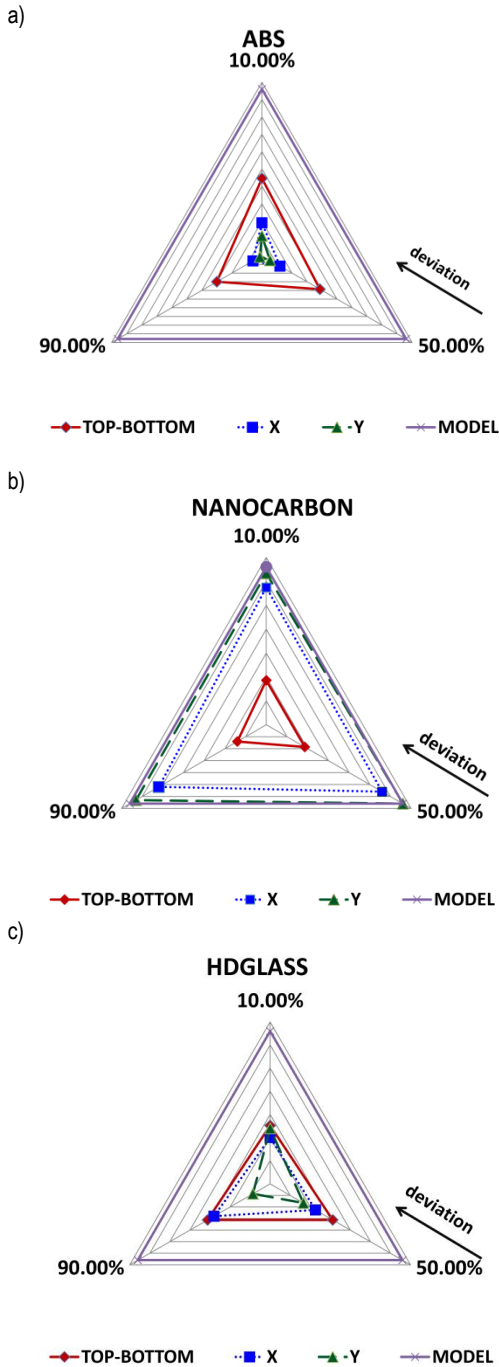


Fig. 10. Effect of infill density on thermal deviations  $\delta$  [mm] for: a) ABS; b) NANOCARBON; c) HDGLASS

The diagrams in Figure 9 show how deviations for individual materials were distributed in directions. The anisotropy of ABS plastic deviations in relation to the tested directions (machine axes) was distinguished.

The analysis of dimensional deviations also shows a special effect of 50% infill density in case of ABS deviations. This degree of infill density results in the greatest change in the size and surface texture parameters. For composite materials, the changes of geometric form were found to have more anisotropic character.



movement of macromolecules, affect nucleation and growth of primary crystalline structures and then promotes the formation of a fully developed crystalline structure with the same cooling rate as in homogeneous plastics.

## 6. CONCLUSIONS

The obtained results can have a cognitive and utilitarian character. The practical aim of the research was to determine the material on the basis of test specimens' measurements, whose properties and application method allow to obtain products of the best quality.

- It was found that the quality of products shaped by FDM technology depends on the type of filament used for building as on the infill density.
- On the process completion, all the printed specimens reduce their volume during cooling, but not equally. The smallest linear shrinkage was found in NANOCARBON specimens, the largest in ABS. The best results were obtained for HDGLASS with an infill density of 90%.
- The description of surface texture with areal parameters gives higher estimates of spatial features. The highest diversity of analysed roughness as well as areal parameters was observed for NANOCARBON.
- The heterogeneous structure of surfaces shaped with the FDM method requires multiparametric evaluation, which was achieved by using two methods of analysing the surface irregularities that together characterize the tested specimens.
- Modification of thermoplastic filament materials by adding fibres may improve not only their mechanical but also geometrical properties of the fabricated parts. The composites studied were characterized by higher resistance to thermal phenomena and smoother surface than ABS monoplatic.
- Further exploring the processability of composites are planned among others by employing thermal analysis.
- Our exploratory research, thanks to the initial recognition of the problem, will allow us to determine the best research project on evaluate of geometric quality of parts fabricated from HDGLASS and NANOCARBON composites.

## REFERENCES

1. **Adamczak S.** (2008), *Surface geometric measurements – in Polish*, WNT, Warszawa.
2. **Al-Hariri L. A., Leonhardt B., Nowotarski M., Magi J., Chambliss K., Venzel T., Delekar S. and Acquah S.** (2016), Carbon Nanotubes and Graphene as Additives in 3D Printing. Carbon Nanotubes, *Current Progress of their Polymer Composites*, 221–251, [https://scholarworks.umass.edu/chem\\_faculty\\_pubs/1448](https://scholarworks.umass.edu/chem_faculty_pubs/1448).
3. **Alsoufi M. S., Elsayed A. E.,** (2018), Surface Roughness Quality and Dimensional Accuracy - A Comprehensive Analysis of 100% Infill Printed Parts Fabricated by a Personal/Desktop Cost-Effective FDM 3D Printer, *Materials Sciences and Applications*, 9, 11–40.
4. **Bähr F., Westkamper E.** (2018) Correlations between Influencing Parameters and Quality Properties of Components Produced by Fused Deposition Modeling, *Procedia CIRP*, 72, 1214–1219.
5. **Barczewski M., Chmielewska D., Sterzyński T., Andrzejewski J.** (2012), The assessment of properties of nucleated isotactic polypropylene modified with silsesquioxanes – in Polish, *Przetwórstwo Tworzyw*, 5, 409–413.
6. **Blok L. G., Longana M. L., Yu H., Woods B. K. S.** (2018), An investigation into 3D printing of fibre reinforced thermoplastic, *Additive Manufacturing*, 22, 176–186.
7. **Calcagnile P., Cacciatore G., Demitri C., Montagna F. and Corcione C. E.** (2018), Fused Deposition Modeling 3D Printer A Feasibility Study of Processing Polydimethylsiloxane–Sodium Carboxymethylcellulose Composites by a Low-Cost Fused Deposition Modeling 3D Printer, *Materials*, 11, 1578, 1–14.
8. **Dikshit V., Nagalingam A., Yap Y. L., Sing S. L., Yeong W. Y. and Wei J.** (2017), Investigation of quasi-static indentation response of inkjet printed sandwich structures under various indenter geometries, *Materials*, 10 (3), 290, 1–18.
9. **Dudek P., Zagórski K.** (2017), Cost, resources, and energy efficiency of Additive Manufacturing, *E3S Web of Conferences*, ISSN 2267-1242, 14, 1–8.
10. **Duo Dong Goh, Yee Ling Yap, Shweta Agarwala, and Wai Yee Yeong** (2019), Recent Progress in Additive Manufacturing of Fiber Reinforced Polymer Composite, *Adv. Mater. Technol.*, 4, WILEY-VCH Weinheim, 856–863.
11. **Golebiowski J.** (2004), Polymer nanocomposites. Structure, synthesis and properties – in Polish. *Przemysł Chemiczny*, 83, 1, 15–20.
12. **Grzesik W.** (2016), Prediction of the Functional Performance of Machined Components Based on Surface Topography: State of the Art, 25(10), 4460–4468.
13. **Guillemot G., Bigerelle M., and Khawaja Z.** (2014), 3D Parameter to Quantify the Anisotropy Measurement of Periodic Structures on Rough Surfaces, *Scanning*, 36, 127–133.
14. **Hashimoto F.** (2016), Characteristics and Performance of surface created by various finishing methods, *Procedia CIRP*, 45, 1–6.
15. **Hofstätter T., Pedersen, Bue D., Tosello G., Nørgaard H.** (2019), State-of-the-art of fiber-reinforced polymers in additive manufacturing technologies, *Journal of Reinforced Plastics & Composites*, 36(15), 1061–1073.
16. **ISO/ASTM 52900:2015**, Additive manufacturing – General principles – Terminology.
17. **Kaczyński R., Wilczewska I., A. Sfiridienok** (2014), Peculiarities of the wear mechanism of polymers reinforced with unidirectional carbon fibers, *Friction and Wear*, 35 (6), 449–454.
18. **Knoop F., Kloke A., and Schoeppner V.** (2018), Quality improvement of FDM parts by parameter optimization, *AIP Conference Proceedings*, 190001-1–190001-5.
19. **Kumar S., Panneerselvam K.** (2016), Two-body Abrasive Wear Behavior of Nylon 6 and Glass Fiber Reinforced (GFR) Nylon 6 Composite, *Procedia Technology*, 25 (2016) 1129–1136.
20. **Kwiatkowski D., Kwiatkowska M.** (2012), Numerical analysis of volume shrinkage of polyacetal composites with glass fibre – in Polish, *Przetwórstwo Tworzyw*, 5, 452–455.
21. **Ligon S.C., Liska R., Stampfl J., Gurr M. and Mulhaupt R.** (2017), Polymers for 3D Printing and Customized Additive Manufacturing, *Chemical Review*, 117, 10212–10290.
22. **Liu Z., Lei Q., Xinga S.** (2019), Mechanical characteristics of wood, ceramic, metal and carbon fiber-based PLA composites fabricated by FDM, *Journal of Materials Research and Technology*, 8(5), 3741–3751.
23. **Loncierz D., Kajzer W.** (2016), Influence of 3D printing parameters in the FDM technology on mechanical and utility properties of objects made of PLA – in Polish, *Aktualne Problemy Biomechaniki*, No. 10, 43–48.
24. **Mathiaa T. G., Pawlus P., Wieczorowski M.** (2011), Recent trends in surface metrology, *Wear*, Vol. 271, No. 3–4, 494–508.
25. **Mohan N., Senthil P., Vinodh S. & Jayanth N.** (2017), A review on composite materials and process parameters optimisation for the fused deposition modelling process, *Virtual and Physical Prototyping*, Vol. 12, No. 1, 47–59.
26. **Nuñez P. J., Rivas A., García-Plaza E., Beamud E., Sanz-Lobera A.** (2015), Dimensional and surface texture characterization in Fused Deposition Modelling (FDM) with ABS plus, *The Manufactur-*

- ing Engineering Society International Conference MESIC 2015, *Procedia Engineering*, 132, 856–863.
27. **Petropoulos G., Pandazaras C. N., Davim P.** (2010), Surface Texture Characterization and Evaluation Related to Machining. Surface Integrity in Machining, *Springer*, 37–66.
  28. **PN-EN ISO 25178-6** (2011), Geometrical product specifications (GPS) — Surface texture: Areal — Part 6: Classification of methods for measuring surface texture – in Polish.
  29. **PN-EN ISO 286-1** (2011), Geometrical product specifications (GPS) – ISO code system for tolerances on linear sizes – Part 1: Basis of tolerances, deviations and fits – in Polish.
  30. **PN-EN ISO 4287:1999/A1** (2010), Geometrical Product Specifications (GPS) - Surface texture: Profile method - Terms, definitions and surface texture parameters – in Polish.
  31. **PN-EN ISO 4288** (1997), Geometrical Product Specifications (GPS) — Surface texture: Profile method — Rules and procedures for the assessment of surface texture - in Polish.
  32. **Prusinowski A., Kaczyński R.** (2017), Simulation of processes occurring in the extrusion head used in additive manufacturing technology, *Acta Mechanica et Automatica*, 11 (4), 317–321.
  33. **Roberson D.A., Shemelya C. M., MacDonald E., Wicker R. B.** (2015), Expanding the Applicability of FDM-type Technologies Through Materials Development, *Rapid Prototyping Journal*, 21 (2), 137–143.
  34. **Singh R., Vatsalya** (2015), Evolution of 3D Surface Parameters: A Comprehensive Survey, *The International Journal of Engineering and Science*, 4 (2), 4–10.
  35. **Spoerk M., Holzer C., Gonzalez-Gutierrez J.** (2019), Material extrusion-based additive manufacturing of polypropylene: A review on how to improve dimensional inaccuracy and warpage, *J. Appl. Polym. Sci*, DOI: 10.1002/app.48545, 1–14.
  36. **Tomić D., Fudurić A., Mihalić T., Simunić N.** (2017), Dimensional accuracy of prototypes made with FDM technology, *Journal of Energy Technology*, 2, 51–59.
  37. **Triantaphyllou A., Giusca C., Macaulay G., Roerig F., Hoebel M., Leach R., Tomita B., Milne K.** (2015), Surface texture measurement for additive manufacturing, *Surface Topography: Metrology and Properties*, 3, 1–8.
  38. **Umaras E., Tsuzuki M. S. G.** (2017), Additive Manufacturing - Considerations on Geometric Accuracy and Factors of Influence, *IFAC PapersOnLine*, 50 (1), 14940–14945.
  39. **Wang T.- M., Xi J.-U., Jin Y.** (2007), A model research for prototype warp deformation in the FDM process, *The International Journal of Advanced Manufacturing Technology*, 33, 1087–1096.
  40. **Wieczorowski M.** (2013), Theoretical basis of spatial analysis of surface asperities – in Polish, *Inżynieria Maszyn*, 18(3), 7–34. [www.formfutura.com](http://www.formfutura.com) (access 07.09.2019).
  41. [www.markforged.com](http://www.markforged.com) (access 07.09.2019).
  42. [www.rp-tech.pl](http://www.rp-tech.pl) (access 07.09.2019).
  43. **Zabala A., Blunt L., Wilson W., Aginagalde A., Gomez X. and Mondragon I. L.** (2018), The use of areal surface topography characterisation in relation to fatigue performance, *MATEC Web of Conferences*, 165, 1–6.
  44. **Zawistowski H.** (2008), Basics of the theory of shaping the properties of products in the process of injection of thermoplastics – in Polish, *Mechanik*, 4, 274–280.
  45. **Żuchowska D.** (2000), *Constructional polymers* – in Polish, WNT, Warszawa